



Fabrication and magnetic properties of cobalt nanorod arrays containing a number of ultrafine nanowires electrodeposited within an AAO/SBA-15 template

Guangbin Ji^{a,*}, Zhihong Gong^a, Yousong Liu^a, Xiaofeng Chang^a, Youwei Du^b, M. Qamar^c

^a Department of Applied Chemistry, College of Material Science and Technology, Nanjing University of Aeronautics and Astronautics, Nanjing 211100, PR China

^b National Laboratory of Solid State Microstructure and Physics Department of Nanjing University, Nanjing 210093, PR China

^c Center of Excellence in Nanotechnology (CENT), King Fahd University of Petroleum and Minerals, Dhahran 31261, Saudi Arabia

ARTICLE INFO

Article history:

Received 5 October 2010

Received in revised form

4 April 2011

Accepted 11 May 2011

by D.J. Lockwood

Available online 19 May 2011

Keywords:

A. Mesoporous Co nanoarrays

B. AAO/SBA-15 composite templates

C. Electrodeposition

ABSTRACT

Arrays of cobalt nanorods consisting of a number of nanowires have been fabricated by the electrochemical method using an anodic-aluminum oxide (AAO)/mesoporous-silica (SBA-15) composite. Microscopic studies clearly display that each nanorod (with a diameter of ~ 200 nm) of the array was consisting of a number of cobalt nanowires which exhibit an average diameter of 3 nm. The observed hysteresis loops measured at room temperature indicate that the magnetic shape anisotropy of cobalt mesostructures, i.e. the parallel and perpendicular squarenesses of 0.5 and 0.1, respectively have been estimated. The maximum value of the coercivity measured perpendicular to the sample axis shows a value of 330 Oe and it was found that the coercivity decreases by increasing the temperature which is possibly caused by thermal disturbance inside the arrays.

Crown Copyright © 2011 Published by Elsevier Ltd. All rights reserved.

1. Introduction

Iron (Fe), cobalt (Co) and nickel (Ni) magnetic nanomaterials with 1-D structure have significant importance in fundamental research as well as in potential technological applications such as magnetic recording media, sensors and other devices [1–3]. Due to the high aspect ratio and self-ordered hexagonal pore structure, anodic aluminum oxide (AAO) templates have been extensively studied considering the growth of ordered 1-D nanostructures within their pores [4,5]. The synthesis of cobalt nanowire arrays with 1-D structure using an AAO template have been reported in the scientific literature. Huang et al. prepared the arrays of cobalt nanowires with controlled diameters and identical lengths of 40 nm by a pulsed electrodeposition method [6]. Ren et al. fabricated cobalt nanowire arrays with a length of ~ 20 nm with a high coercivity of 1360 Oe through alternating-current (AC) electrodeposition [7]. It is worth noticing that the AAO templates have a wide range of porosity starting from some nanometers to several hundred nanometers. However, the lack of smaller pores (a few nanometers) in AAO templates limits their application in the preparation of 1-D nanomaterials having smaller diameters which are being applied for the fabrication of nanodevices with high efficiencies and bioseparation of small molecules.

Recently, mesoporous materials having unique characteristics such as narrow pore size distribution, high specific surface area, high pore volume etc, have received particular attention in various research areas including hydrogen storage [8], separation [9], catalysis [10] etc. Efforts have been made to develop mesoporous materials such as non-metallic mesoporous silica [11], mesoporous carbon nano-filaments [12], mesoporous titania [13] etc. Among many mesoporous materials, ordered mesoporous silica has attracted much attention because of the highly ordered hexagonally arranged mesochannels, thick walls of ~ 2 nm [14], adjustable pore size and high thermal stability [15]. Since the pore size of mesoporous silica is smaller than that of AAO, it offers many advantages especially the quantum size effect. It has been shown that the combination of AAO and mesoporous silica results in the formation of new hierarchical structures where the advantages of both the templates are utilized [16–19]. It has been found that the SBA-15 mesostructures can be directed by the pores of alumina membranes to form hexagonal arrays when they were filled in AAO pores. Thus the fine and vertical mesochannels (namely, parallel to the channels of the alumina membrane) which have the characteristics of a narrow pore size distribution, varieties of mesochannels, high specific surface area and a high pore volume can be effectively provided or obtained. Furthermore, in comparison to the materials prepared using AAO as a template under identical conditions, such mesoporous materials synthesized using mesoporous silica as a template have many evident advantages such as higher specific surface area, adjustable morphology etc [20,21].

* Corresponding author. Tel.: +86 25 52112902; fax: +86 25 52112626.

E-mail address: gbjj@nuaa.edu.cn (G. Ji).

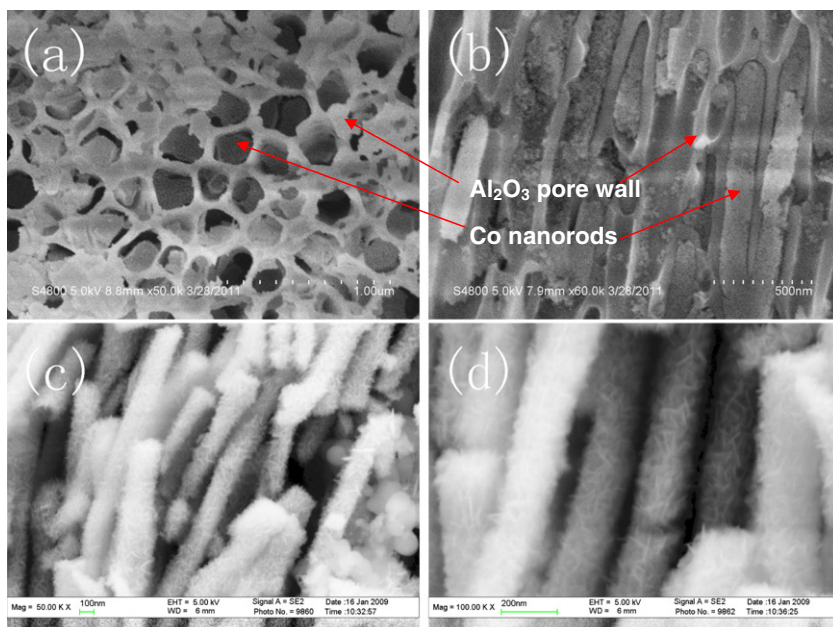


Fig. 1. Typical SEM images of AAO/SAB-15 template after electrodeposition: (a) top view, (b) side view and cobalt nanorods (c, d).

Therefore, such mesoporous composite materials might have great potential in various research fields such as spectroscopy, electronic transmission and magnetic resolution, adsorption or carrier of adsorbent etc. Recently, nanowires of Ag, Ni, and Cu_2O with unprecedented mesostructures, such as coaxially multilayered stacked-donuts, single- and double-helices within the pores of the mesoporous silica, have been successfully prepared [22].

In the present investigation, an attempt has been made to synthesize arrays of cobalt nanorods consisting of a number of nanowires using AAO/SBA-15 as a template by the AC-induced electrodeposition process. The phase structure and morphology was clearly confirmed by means of X-ray diffraction (XRD), field emission scanning electron microscopy (FE-SEM) and transmission electron microscopy (TEM). The magnetic properties (such as perpendicular/parallel coercivity and squarenesses (M_R/M_s)) of as-prepared cobalt nanorod arrays as a function of testing temperature were systematically investigated by using a vibrating sample magnetometer (VSM).

2. Experimental section

2.1. Synthesis

The preparation of the composite template has been described in detail in our previous published literature [23]. Briefly speaking, the aluminum foils, after polishing by the electrochemistry method, were anodized in aqueous solution (0.36 M H_3PO_4) under a constant voltage of 120 V at 0 °C. Subsequently, the pores of the AAO templates were widened in H_3PO_4 (0.3 M) for 3 h. To prepare the precursor (sol) of SBA-15, 0.6 g of poly(ethylene oxide)-b-poly(propylene oxide)-b-poly(ethylene oxide) block copolymer $\text{EO}_{20}\text{PO}_{70}\text{EO}_{20}$ (PEO-PPO-PEO, Pluronic P123) was dissolved in 40 mL ethanol followed by the addition of tetraethyl orthosilicate (TEOS, 0.97 g) and aqueous hydrochloric acid (HCl, 0.4 g) to the mixture, which was stirred for 2 h at room temperature to form the sol [24]. The AAO templates were immersed in the sol for 24 h to ensure a complete infiltration of SBA-15. The membrane was taken out from the sol and the residual sol on the membrane surface was completely scratched away. The final AAO/SBA-15 composite template was produced after the membranes were dried at 60 °C

for 12 h and calcined at 400 °C for 3 h. The electrodeposition was carried out at 25 °C with a current density of 0.5–1.0 mA/cm^2 (AC, 50 Hz) using graphite and an AAO/SBA-15 composite template as the counter-electrode and working electrode, respectively. The aqueous solution composed of $\text{Co}(\text{Ac})_2 \cdot 4\text{H}_2\text{O}$ (0.1 M) and H_3BO_4 (0.2 M) was employed as the electrolyte and the deposition time was controlled to be between 6 and 12 h.

2.2. Characterization

The magnetic properties were measured by a VSM (Lakeshore, Model 7400 series and VersaLab, Quantum Design) with the applied field either perpendicular or parallel to the samples axis. The morphology of as-prepared samples was observed by FE-SEM (Hitachi S-4800 and Gemini LEO 1530) and TEM (JEOL JEM 2100). For the FE-SEM observation, small pieces of AAO/SBA-15 with cobalt nanorod arrays were eroded slightly by an aqueous solution of NaOH (2 M) at room temperature. The samples were then cleaned with distilled water for several times. For the TEM (including high resolution TEM, HR-TEM) observation, the AAO/SBA-15 composite template was immersed in 4 M NaOH for 4 days at room temperature in order to release the cobalt nanomaterials from the composite template. A small drop of suspension was placed on copper grids covered with a carbon thin film. The phase structure of as-prepared samples was examined by means of X-ray diffraction (XRD) using $\text{Cu-K}\alpha$ as the X-ray source ($\lambda = 0.15418 \text{ nm}$) with a voltage of 40 kV and a current of 100 mA, respectively.

3. Results and discussion

3.1. Morphology and structural properties

A top view FE-SEM image of the AAO/SBA-15 composite template is depicted in Fig. 1(a) whose pore diameter was measured to be around 200 nm. It was observed that most of the AAO nanochannels were filled with silica nanofibers exhibiting a mesostructure. Fig. 1(b) shows the side view of the AAO/SBA-15 composite template, from which it can be seen that the cobalt nanorods grew in the AAO nanochannels and were oriented vertically to the AAO membrane. Fig. 1(c) and (d) shows the arrays of as-electrochemical-deposited cobalt nanorods. From the

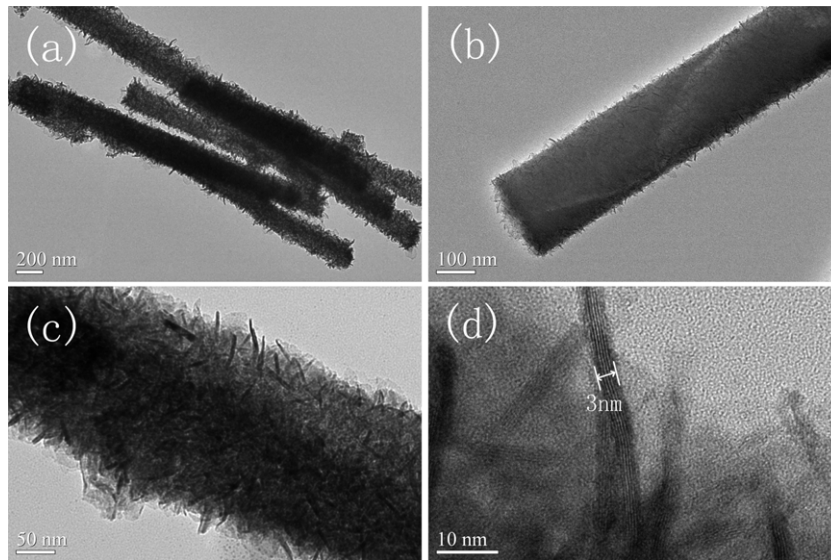


Fig. 2. Typical TEM images of as-prepared cobalt nanorod arrays detached from AAO/SBA-15 template: (a) a bundle of nanowires; (b) and (c) a single nanowire; and (d) representative HR-TEM image.

FE-SEM images, the diameter of the nanorods was estimated to be around 200 nm. The cobalt nanorods, Fig. 1(b) tend to accumulate and were seen to be broken partially upon the removal of the template. Additionally, the mass or amount of nanowires existing in the nanorods can be estimated based on the FE-SEM observation. In order to get further insight, samples were also analyzed by means of TEM and a typical TEM image of the as-prepared samples is depicted in Fig. 2. From Fig. 2(a) and (b), the length and average diameter of the synthesized nanorods were measured to be around 3 μm and 200 nm, respectively. The magnified TEM image (Fig. 2(c)) clearly showed that each cobalt nanorod consisted of a number of nanowires which grew irregularly, possibly caused by the mesoporous structure of SBA-15. As the silica grew with a self-assembly mechanism, the channels of SBA-15 crossed each other and formed a network structure which made the cobalt grains grow along different directions in the meantime. A representative HR-TEM image depicted in Fig. 2(d) further demonstrated that the diameter of the disordered nanowire was about 3 nm.

Fig. 3 depicts the XRD pattern of cobalt nanorod arrays which were prepared using the AAO/SBA-15 composite as a template. The diffraction peak around 38.65° was indexed to the hexagonal structure (space group: $P63/mmc$) of cobalt (JCPDS card no. 05-0727) which corresponds to the crystal indexes of (311). In addition, two apparent diffraction peaks with strong intensity, corresponding to the (220) and (311) crystal indexes of aluminum around 65.13° and 78.30° , were observed because the Al substrate was not removed. It was difficult to characterize the diffraction peak around 44.78° because it resulted either from the crystal indexes (002) of cobalt or (200) of the Al substrate. However, the crystal structure investigation revealed the preferential orientations of (311) and/or (002) for as-deposited Co nanocrystals as the strong confinement of the porous wall during the crystal growth within the pores of the SBA-15/AAO composite.

3.2. Magnetic properties

The magnetic properties of as-prepared arrays were studied by VSM. Fig. 4 presents the hysteresis loops ($M-H$ loops) of the as-deposited typical cobalt nanorod arrays with the external magnetic field parallel and perpendicular to the sample axis measured at

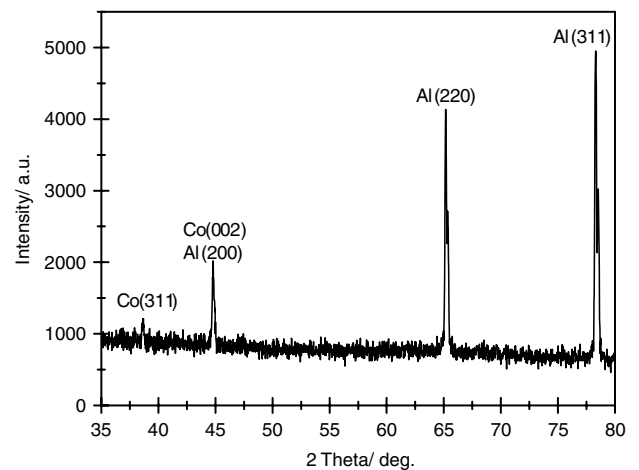


Fig. 3. The XRD pattern of as-prepared cobalt nanorod arrays within the AAO/SBA-15 template.

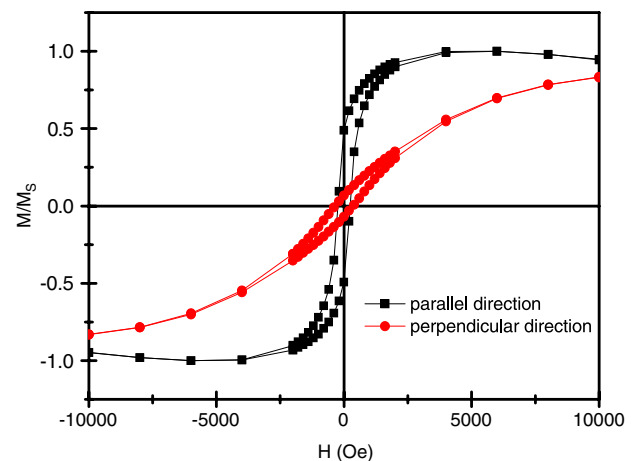


Fig. 4. Typical hysteresis loops of the mesoporous Co nanorods measured at room temperature.

room temperature (300 K). The magnetic coercivity/squareness values were around 250 Oe/0.5 and 330 Oe/0.1, for the induced

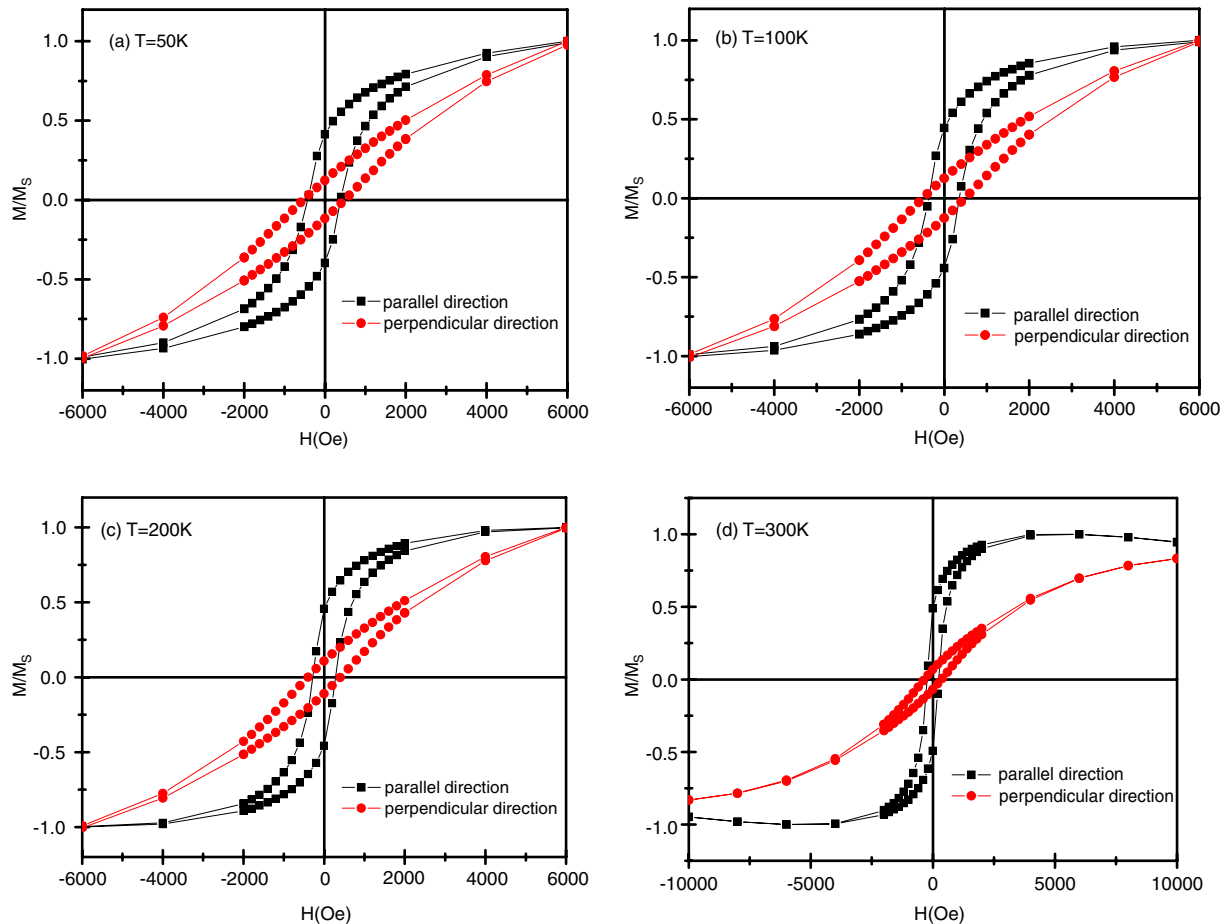


Fig. 5. The M - H loops of cobalt nanorod arrays measured at 50 (a), 100 (b), 200 (c) and 300 K (d).

external magnetic field with directions parallel and perpendicular to the sample axis, respectively. The results mentioned above clearly demonstrated the strong shape anisotropy of the cobalt nanorod arrays.

The M - H loops of as-deposited cobalt nanorod arrays measured at 50, 100, 200 and 300 K are presented in Fig. 5 and the results indicated little difference between the parallel and perpendicular coercivity values. However, the observed much larger parallel squareness showed that the easy axis was along the axis of the nanorods.

Fig. 6 depicts the changes in coercivity and squareness as a function of testing temperature. Both the parallel and perpendicular coercivity were found to decrease with the increase in the measuring temperature and the maximum values were found to be around 490 and 360 Oe, respectively. It is well known that the ferromagnetic materials become paramagnetic when the temperature is high enough, which is referred to as the Curie temperature (T_c), while the cobalt shows ferromagnetism below the temperature of 1404 K (as shown in Fig. 6). Under the external magnetic field, the movement rate of molecules increases with the increase in temperature, below the temperature which is lower than T_c . The thermal perturbation will partly damage the ordered arrangement of magnetic moments within the magnetic domain and hence the spontaneous magnetization was decreased. If the temperature continues to increase up to T_c , the exchange coupling between two neighboring atoms (or molecules) will disappear suddenly, the magnetic domain disappears as well, and the ferromagnetism changes to paramagnetism. From the measured magnetic values, it is reasonable to deduce that the cobalt nanorods

overcame the magnetic anisotropy under the interaction of an external magnetic field and internal heat disturbance. Under identical conditions, the magnetic anisotropy of the particles is certain as the thermal disturbance is proportional to the temperature. But the thermal fluctuation gets smaller when the temperature drops and this phenomenon requires a greater magnetic field strength to help to overcome the magnetic anisotropy energy, resulting in the larger coercivity. The maximum coercivity was, therefore, found at 50 K. Fig. 6(b) depicts the difference of the changes between parallel and perpendicular squareness. The parallel squareness increased slowly while the perpendicular to the wire axis decreased as the testing temperature was increased. The small difference of coercivity values along the two directions can be attributed to the disordered cobalt nanowires. Squareness is another parameter in hysteresis loops which is an indicator of the direction of easy magnetization. As the temperature increases, the magnetization easy axis turned in the direction parallel to the wire axis. This indicated that easy axis magnetization is no longer the direction of nanowires at low temperature.

4. Conclusions

In this present study, arrays of cobalt nanorods (with diameters of ~ 200 nm) consisting of a number of nanowires (with the diameter distribution of 3 nm) were successfully prepared by the electrodeposition method using the AAO/SBA-15 composite as a template. The shape anisotropy of as-prepared Co nanoarrays was determined based on the magnetic results. The maximum parallel

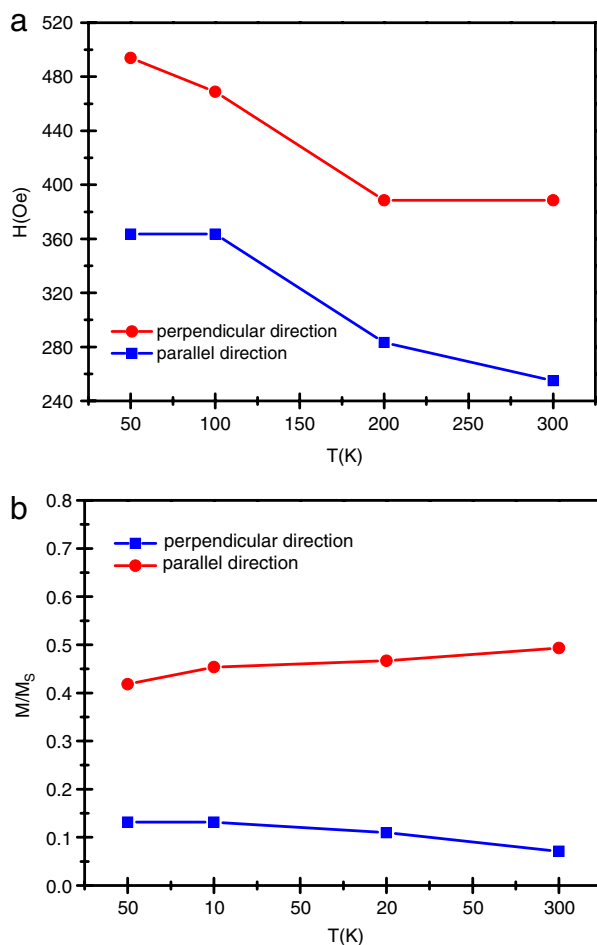


Fig. 6. The variations in coercivity (a) and squareness (b) of cobalt nanorod arrays as a function of testing temperature.

and perpendicular coercivity values of as-prepared samples were measured at 490 and 360 Oe (at 50 K), respectively. The coercivity

of as-prepared cobalt nanorod arrays was decreased with the increase in temperature is possibly due to the thermal disturbance inside the arrays.

Acknowledgment

Financial support from the National Natural Science Foundation of China (50701024) and Natural Science Foundation of Jiangsu Province of China (No: BK2010497) are gratefully acknowledged.

References

- [1] M.S. Sander, A.L. Prieto, R. Gronsky, T. Sands, A.M. Stacy, *Adv. Mater.* 14 (2002) 665.
- [2] F. Wacquant, S. Denolly, J.P. Nozieres, D. Givord, V. Mazauric, *J. Appl. Phys.* 85 (1999) 5483.
- [3] L.C. Sampaio, E.H.C.P. Sinnecker, G.R.C. Cernicchiaro, M. Knobel, M. Vazquez, J. Velazquez, *Phys. Rev. B* 61 (2000) 8976.
- [4] W.A. de Heer, A. Chatelain, D. Ugarte, *Science* 270 (1995) 1179.
- [5] S. Fan, M.G. Chapline, N.M. Franklin, T.W. Tomblor, A.M. Cassell, H. Dai, *Science* 283 (1999) 512.
- [6] X.H. Huang, G.H. Li, X.C. Dou, L. Li, *J. Appl. Phys.* 105 (2009) 084306.
- [7] Y. Ren, Q.F. Liu, S.L. Li, J.B. Wang, X.H. Han, *J. Magn. Magn. Mater.* 321 (2009) 226.
- [8] L. Li, X.D. Yao, C.H. Sun, A.J. Du, L.N. Cheng, Z.H. Zhu, C.Z. Yu, J. Zou, S.C. Smith, P. Wang, H.M. Cheng, R.L. Prost, G.Q. Lu, *Adv. Funct. Mater.* 19 (2009) 265.
- [9] Y.L. Dong, B. Lu, S.Y. Zang, J.X. Zhao, X.G. Wang, Q.H. Cai, *J. Chem. Technol. Biotechnol.* 86 (2011) 616.
- [10] Z.H. Wen, J. Liu, J.H. Li, *Adv. Mater.* 20 (2008) 743.
- [11] Y.K. Anthony, T.T. Seth, M.L. Sergio, *J. Am. Chem. Soc.* 127 (2005) 6934.
- [12] D.J. Cott, N. Petkov, M.A. Morris, B. Platschek, T. Bein, J.D. Holmes, *J. Am. Chem. Soc.* 128 (2006) 3920.
- [13] S. Madhugiri, B. Sun, P.G. Smirniotis, J.P. Ferraris, J. Balkus, *Micropor. Mesopor. Mater.* 69 (2004) 77.
- [14] M. Colilla, F. Balas, M. Manzano, M. Vallet-Regi, *Chem. Mater.* 19 (2007) 3099.
- [15] S. Madhugiri, A. Dalton, J. Gutierrez, J.P. Ferraris, K.J. Balkus, *J. Am. Chem. Soc.* 125 (2003) 14531.
- [16] Q. Lu, F. Gao, S. Komarneni, et al., *J. Am. Chem. Soc.* 126 (2004) 8650.
- [17] Y. Akira, U. Fumiaki, Y. Takashi, et al., *Nature Mater.* 3 (2004) 337.
- [18] Z.J. Liang, A.S. Susha, *Chem. Eur. J.* 10 (2004) 4910.
- [19] Y.Y. Wu, G.S. Cheng, K. Katsov, *Nature Mater.* 3 (2004) 816.
- [20] D.S. Wang, T. Xie, Q. Peng, Y.D. Li, *J. Am. Chem. Soc.* 130 (2008) 4016.
- [21] J.K. Shon, S.S. Kong, J.M. Kim, *Chem. Commun.* 6 (2009) 650.
- [22] G.D. Stucky, *Nano Lett.* 4 (2004) 2337.
- [23] Z.H. Gong, G.B. Ji, M.B. Zheng, X.F. Chang, W.J. Dai, L.J. Pan, Y. Shi, Y.D. Zheng, *Nanoscale Res. Lett.* 4 (2009) 1257.
- [24] H. Yang, Q. Shi, B. Tian, S. Xie, Zhang, F.Y. Yan, B. Tu, D. Zhao, *Chem. Mater.* 15 (2003) 536.